We are IntechOpen, the world's leading publisher of Open Access books Built by scientists, for scientists

6,900
Open access books available

185,000
International authors and editors

200M
Downloads

Our authors are among the

154
Countries delivered to

TOP 1%
most cited scientists

12.2%
Contributors from top 500 universities



WEB OF SCIENCE™

Selection of our books indexed in the Book Citation Index in Web of Science™ Core Collection (BKCI)

Interested in publishing with us?
Contact book.department@intechopen.com

Numbers displayed above are based on latest data collected.
For more information visit www.intechopen.com



2

Nucleation and Vertical Growth of Nano-Graphene Sheets

Hiroki Kondo, Masaru Hori and Mineo Hiramatsu
Nagoya University, Meijo University
Japan

1. Introduction

Carbon nanomaterials, such as carbon nanotubes (CNTs), graphene sheets and so forth, have attracted much attention for not only scientific interest but also various application expectations. For example, various applications of CNTs, such as field emitter, transistor channel, and so forth, have been proposed, because of their unique nanostructures, excellent electrical and physical properties.[1-3] Graphene sheets are also promising candidates as channel materials of electronic devices, since both electron and hole in them have extremely high carrier mobilities (10,000–15,000 cm^2/Vs).[4] Carbon nanowalls (CNWs) are one of such self-aligned carbon nanomaterials. They consist of graphene sheets standing vertically on substrates as shown in Fig.1. Significant recent attention has been focused on the functionalities of CNWs for future devices because of their unique morphologies and excellent electrical properties. For example, since they have large surface-to-volume ratios and very high aspect ratios, they are expected as catalyst supporting materials in fuel cells, field emitters, and various kinds of templates [5-7]. In addition, the recent reports of extremely high carrier mobilities in graphene sheets suggest that the CNWs would also possess excellent electrical properties. Therefore, the CNWs are also expected to be applied to high-carrier-mobility channels and low-resistivity electrodes in next-generation electronic devices.

For the practical applications of CNWs, it is indispensable to control their morphologies and electrical properties. And, to establish such the controlled synthesis techniques of CNWs, it is essential to clarify their growth mechanisms. For the synthesis of the CNWs, the plasma-enhanced chemical vapor deposition (PECVD) systems are used in most cases and no catalyst is necessary for its growth [5-11]. However, their growth mechanisms have not been sufficiently clarified yet. Tachibana et al. reported interesting results of crystallographic analysis on carbon nanowalls, in which preferential orientations of graphene sheets change with the growth time.[12] On the other hand, more fundamental mechanisms of CNW growth, such as nucleation of nanographene, and relationships between plasma chemistry and CNW growth, are poorly understood. It is due to the complicated growth processes in the plasma. In this study, we investigated roles of radicals and ions in the growth processes of CNWs by distinctive inventions on the originally-developed Multi-beam PECVD systems and precise measurements of active species during the growth processes.

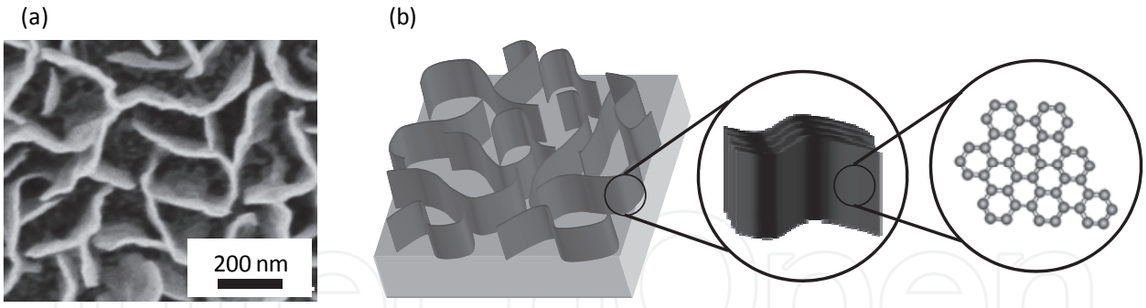


Fig. 1. (a) Top-view SEM image and (b) schematic illustrations of typical CNWs.

2. Initial growth processes of carbon nanowalls

When the growth of the CNWs is performed by the PECVD for different growth times, it can be found that there are the series of events leading up to the formation of CNWs. A 10 nm thick interface layer composed of carbon nanoislands was firstly formed on the Si substrate for a short time, and then CNWs growth began from the nuclei on the interface layer [13]. In order to realize the industrial applications of CNWs with unique characteristics, it is very important to understand the growth mechanism of the initial layer and CNWs to achieve control of the characteristics and morphologies that are appropriate to each application [5-7]. Moreover, the nucleation of CNWs in the very early phase must be very important for control of the characteristics and morphology. The following questions to be solved are; why are the morphologies changed from an interface layer (nanoislands) to CNWs under homogeneous conditions, and why do vertical CNWs grow from flat interface layers. To answer these questions, the surface conditions suitable for CNW growth were investigated using a multi-beam chemical vapor deposition (CVD) system and the correlation between the nanoislands and CNW growth was investigated.

A rapid and simple preparation process is desirable for industrial applications. On the other hand, it is also very important to separate each growth phase, formation of the nanoislands, nucleation, and CNW growth, to elucidate these mechanisms. However, it is difficult to separate these growth phases because the formation of nanoislands and nucleation proceed within a very short duration with plasma-enhanced CVD (PECVD). Moreover, the conditions for nanoisland formation and nucleation are almost the same as that of the subsequent CNW growth. Therefore, we have focused on the early phases, and established two different conditions for nanoisland formation and CNW growth starting with the first incidence of graphene (nucleation). In this study, a pretreatment was introduced for the formation of nanoislands, and the effects of the pretreatment process on CNW growth were investigated. CNWs are grown on an amorphous carbon (a-C) interface layer including the nanoislands. The optimum surface conditions for nucleation of CNWs are discussed in the latter section.

2.1 Multi-beam chemical vapor deposition system and two-step growth technique

As mentioned above, the nucleation of nanographene occurs at the very early phase of CNWs growth generally. Therefore, it is very difficult to detect it when we use the conventional PECVD system. In addition, it is also hard to clarify roles of each radicals or ions at the PECVD processes, since fluxes and energies of each active species are not

independently-controllable in the conventional PECVD system. Therefore, in this study, we employed the multi-beam CVD system having independently-regulated two radial sources and one ion source. Using this system, the effects of each active species on nucleation and vertical growth of nanographene during the formation of the CNWs can be systematically evaluated.

2.1.1 Multi-beam chemical vapor deposition system

Figure 2 shows the schematic diagram of multi-beam CVD system. This system consists of 3 beams of carbon-containing radicals, hydrogen radicals, and ions.[14] Two radical sources (fluorocarbon and H radicals) were mounted obliquely at the upper right and left sides of the reactive chamber, and C_2F_6 and H_2 gases were introduced into the radical sources separately. The identical radical sources consist of radio frequency (rf: 13.56 MHz) inductively coupled plasma (ICP) with spiral coil and grounded metal meshes in the head to retard irradiating electrons and ions. Orifices were installed in the head of fluorocarbon radical source and H radical source, respectively, in order to control the flux of radicals. Radicals generated in these sources irradiated a substrate with the angle of 30° from the horizontal line. On the other hand, the ion source was mounted on the top of the reactive chamber. The ion source consists of 13.56 MHz rf ICP. The plasma potential in the ICP was set to 0–250 V by applying DC voltage. A metal mesh connecting to the ground was installed inside the ion source. Generated Ar^+ ions were accelerated between the ICP and the mesh, and irradiated vertically a substrate. The ion current is measured using Faraday cup.

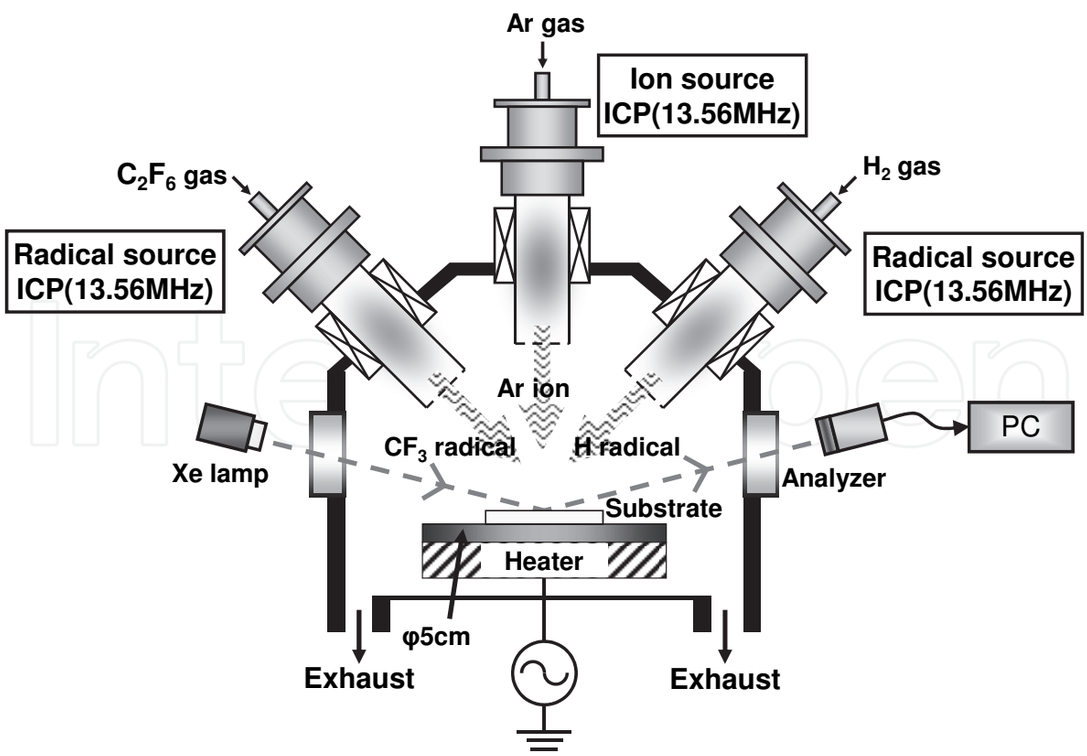


Fig. 2. Schematic diagram of multi-beam CVD system.[13]

The process gases and irradiated active species are pumped out by a turbo molecular pump, and the total pressure is controlled by a gate valve. The base pressure was approximately 1.0×10^{-4} Pa. A substrate is introduced onto the stage in the center of the chamber, where irradiations of all species were focused on. When CNWs are synthesized, the substrate is heated by a carbon heater beneath the lower electrode and the substrate temperature is measured by an optical pyrometer and ellipsometric analysis. In-situ spectroscopic ellipsometry is available in this system. Xe lamp and the detector were installed on the windows in the side wall of the chamber in opposed position with the angle of 15° from the horizontal line. This spectroscopic ellipsometer would obtain some information of the growing materials in real time. Measured ellipsometric data were calculated and fit by using a personal computer.

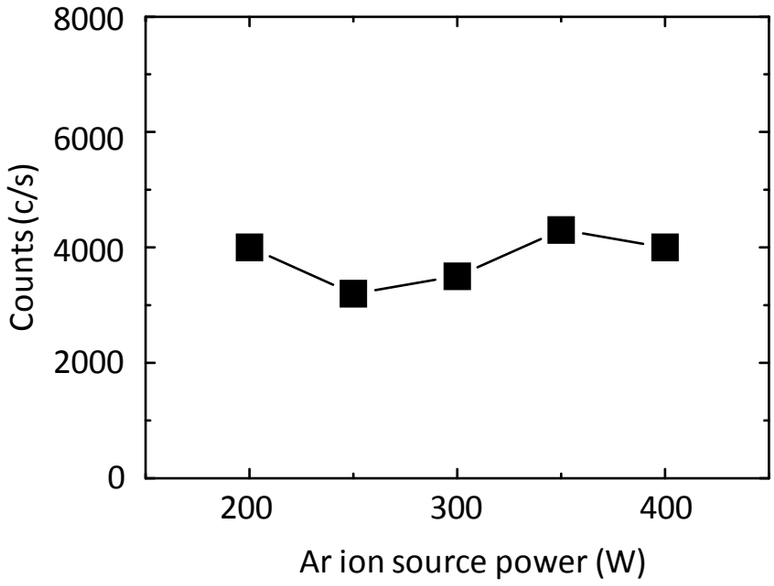


Fig. 3. Counts of CF_3^+ ions ionized from CF_3 radicals as a function of Ar^+ ion source power.

Independent controllability of this system was confirmed by quadrupole mass spectrometry (QMS).[15-17] Figure 3 shows the signal (counts) of CF_3^+ ion ionized from CF_3 radicals obtained by QMS as a function of rf-ICP power of Ar^+ ion source. The intensity did not significantly change. Any other relations such as fluorocarbon radical vs H radicals showed the similar behaviours. From the result, the irradiations can be independently controlled.

2.1.2 Two-step growth technique

CNW growth was carried out using the multi-beam CVD system. Two different deposition sequences for CNW growth were performed and are indicated in Table 1. The first is a single-step growth with constant irradiation conditions of the Si substrates (no pretreatment), and the second is a two-step growth on Si substrate. In the two-step growth, the first step is a 15 min pretreatment and the second step is CNW growth for 35 min, wherein the gas flow rate, ICP power, and Ar^+ ion acceleration voltage and flux are varied. The Ar^+ flux in the second step was varied from 1.8 to 5.4 $\mu A/cm^2$ by changing the ICP power, and the ion energy was varied from 160 to 250 eV by changing the DC voltage. Combinations of irradiation with fluorocarbon radicals, H radicals, and Ar^+ ions were

varied in the pretreatment step. In contrast, the conditions of the second step (subsequent CNW growth) were not changed to analyze the effects of the pretreatment.

		Single-step growth	Two-step growth	
			First (Pretreatment)	Second (Growth)
Total pressure (Pa)		2.5	2.0	2.5
Substrate temperature (°C)		580		
Process time (min)		50	15	35
Flow rate (sccm)	C_2F_6	10	5	10
	H_2	6	6	6
	Ar	5	10	5
ICP power (W)	C_2F_6	200		
	H_2	200		
	Ar	300	300	100–300
Ar^+ ion	Acceleration voltage (V)	200	200	160–250
	Flux ($\mu A/cm^2$)	3.8	1.8	1.8–5.4

Table 1. Growth conditions

C_2F_6, H_2, and Ar gases were used to generate fluorocarbon radicals, H radicals, and Ar^+ ions, respectively. For the pretreatment step, the flow rates of the C_2F_6, H_2, and Ar gases were 5, 6, and 10 sccm, respectively, and the ICP power for the generation of fluorocarbon radicals, H radicals, and Ar^+ ions were 200, 200, and 300 W, respectively. The reflection powers were less than 10% of forward powers. In the fluorocarbon radical source, CF_3 radicals were predominantly generated. The gases with reactive species were pumped out using a turbo molecular pump through a gate valve. During the pretreatment, the total gas pressure ranged between 0.4 and 2.0 Pa, which was dependent on the combination of irradiation species (i.e. no operation of the gate valve between experiments with different variations of irradiation species). Si substrates were introduced to the center of the stage and the surface temperature was kept at 580°C during the 15 min pretreatment process.

After pretreatment, CNW growth was conducted using the multi-beam CVD system under identical conditions. Ar^+ ion, fluorocarbon radical, and H radical sources were also used and generated from Ar, C_2F_6 and H_2 gases, respectively. The powers of each source were 300, 200, and 200 W, respectively, and the flow rates of Ar, C_2F_6, and H_2 were 5, 10, and 6 sccm, respectively. The surface temperature was maintained at 580°C during the 35 min growth process period.

Following the CNW growth process, samples were observed using a scanning electron microscope (SEM). For some samples, scanning tunneling microscopy (STM) was also conducted. Additionally, in situ spectroscopic ellipsometry was performed throughout the pretreatment and the CNW growth processes.

2.2 Initial growth processes of CNWs

Morphological changes of growth surfaces in the initial phase, and their dependence on the growth conditions are discussed in this chapter. Pre-deposition of carbon layers including nanoisland structures and their morphologies are closely-correlated with following growth of CNWs. Especially, effect of Ar^+ ion irradiation on nanoislands formation at the first step are discussed.

2.2.1 Morphological changes of growth surfaces

Figures 4(a) and 4(b) show tilted-view scanning electron microscopy (SEM) images of samples prepared by single-step growth for (a) 15 min and (b) 50 min.[14] In Fig. 5.1(a), several nanoislands approximately 10 nm in diameter and 5 nm in height are evident on the substrate. X-ray photoelectron spectroscopy (XPS) results have shown that these nanoislands are mainly composed of carbon atoms and a small amount of fluorine. In contrast, CNWs were formed after 50 min growth, as shown in Fig. 4(b). Thus, it was confirmed that CNWs were synthesized by the multi-beam CVD system and also by conventional plasma-enhanced CVD.

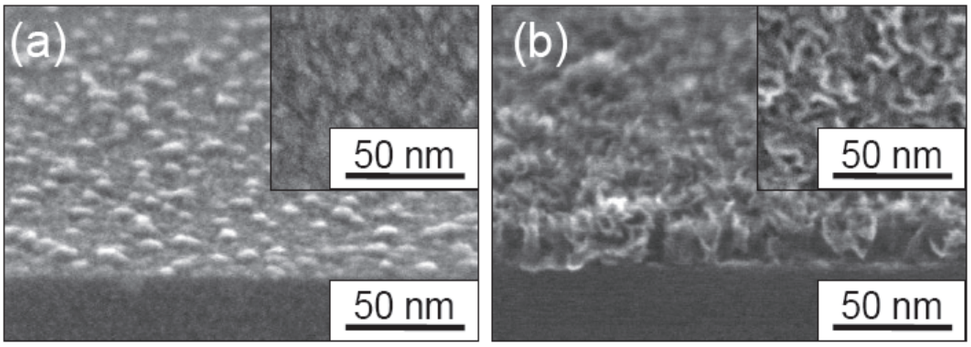


Fig. 4. Tilted-view SEM images of samples formed by single-step growth for (a) 15 and (b) 50 min. Insets show top-view SEM images for each sample.[13]

2.2.2 Effects of nanoislands formation on CNWs growth

Two-step growth was conducted to investigate the nucleation and growth of CNWs separately. Figures 5(a) and (b) show tilted-view STM images of samples after pretreatment with and without Ar^+ irradiation, respectively. In the case of Ar^+ irradiation, nanoislands were observed on the substrate, as shown in Fig. 5(a). Their size and chemical composition were similar to those of the nanoislands shown in Fig. 4(a). In contrast, no nanoislands were obtained without Ar^+ irradiation (Fig. 5(b)). It should be noted that CNWs were never obtained during the pretreatment step, even if performed with or without Ar^+ irradiation for 50 min, which indicates that the irradiation conditions of the ions and radicals required for CNW growth are different from those for nanoisland formation. Figures 5(c) and (d) show tilted-view SEM micrographs of samples grown by the two-step process, where the first step pretreatments were performed with and without Ar^+ irradiation, as shown in Figs. 5 (a) and (b), respectively, and where in the second step, the Ar^+ flux was increased to 3.8 $\mu A/cm^2$ at an energy of 200 eV under the same densities of H and CF_3 radicals as those for single-step growth. It is significant that CNWs are only grown (Fig. 5(c)) when Ar^+ irradiation is used in

the pretreatment step, while only a continuous film was obtained for growth after pretreatment without Ar^+ irradiation (Fig. 5(d)). These results indicate that energetic Ar^+ irradiation during the pretreatment (initial growth process) is necessary for CNW growth, and the nucleation of CNWs is incubated in the nanoislands by high density Ar^+ irradiation. Therefore, nucleation and CNW growth could be clearly distinguished using the two-step growth technique.

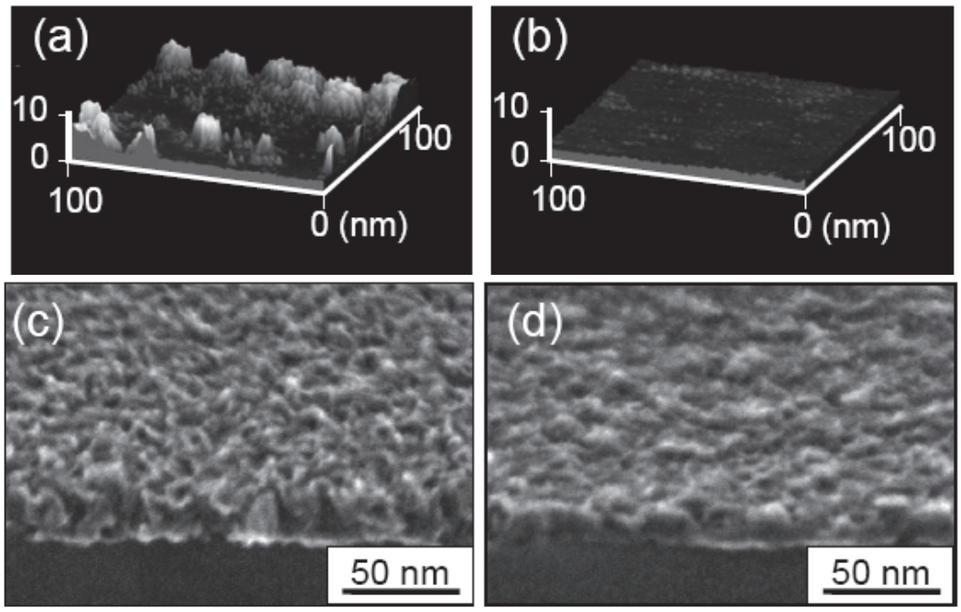


Fig. 5. Tilted-view STM images of samples after pretreatment for 15 min (a) with and (b) without Ar^+ irradiation. Tilted-view SEM images of samples formed by two-step growth, in which pretreatments were performed (c) with and (d) without Ar^+ irradiation.[14]

2.3 Effects of H radicals on CNW growth

The effects of radicals were investigated in a multi-beam CVD system. The H_2 gas flow rate was changed from 0 to 10 sccm in the second step (CNW growth), and C_2F_6 and Ar gas flow rates were kept constant at 10 and 5 sccm, respectively. Therefore, several different composition ratios of H/C or H/CF_3 would be obtained under these conditions. The chamber was evacuated through a gate valve using a turbo molecular pump, and the total gas pressure was controlled at 2.5 Pa by the valve when the H_2 gas flow rate was 5 sccm. The valve position was not changed at various H_2 gas flow rates in order to maintain the fluxes of Ar^+ ions and CF_x radicals. Therefore, the total pressures ranged from 2.2 to 2.8 Pa at H_2 flow rates from 0 to 10 sccm. The rf ICP powers applied to H radical source, fluorocarbon source, and Ar^+ ion source were 200, 200, and 300 W, respectively. The irradiation period for each sample was 35 min.

2.3.1 Morphological dependence of CNWs on H radicals

Figures 6(a)–(e) show tilted-view SEM images of CNWs synthesized for 35 min at different H_2 gas flow rates of (a) 0, (b) 3, (c) 5, (d) 7, and (e) 10 sccm. When the H_2 gas flow rate was 0

sccm, the ICP power for H radical generation was not applied. No CNWs were formed without irradiation by H radicals, but a very thin layer was apparent on the Si substrate, as shown in Fig. 6(a). Figure 6(b) shows that for a H_2 gas flow rate of 3 sccm, nanoparticles rather than CNWs were deposited. In contrast, when the H_2 gas flow rate was increased up to 5 sccm, CNWs were densely grown during the initial phase. In these samples, the distance between adjacent CNWs was approximately 10 to 20 nm, and the thickness of the CNW sheet was less than 5 nm. With further increase of the H_2 gas flow rate to more than 10 sccm, no CNWs were grown, as shown in Fig. 6(e).

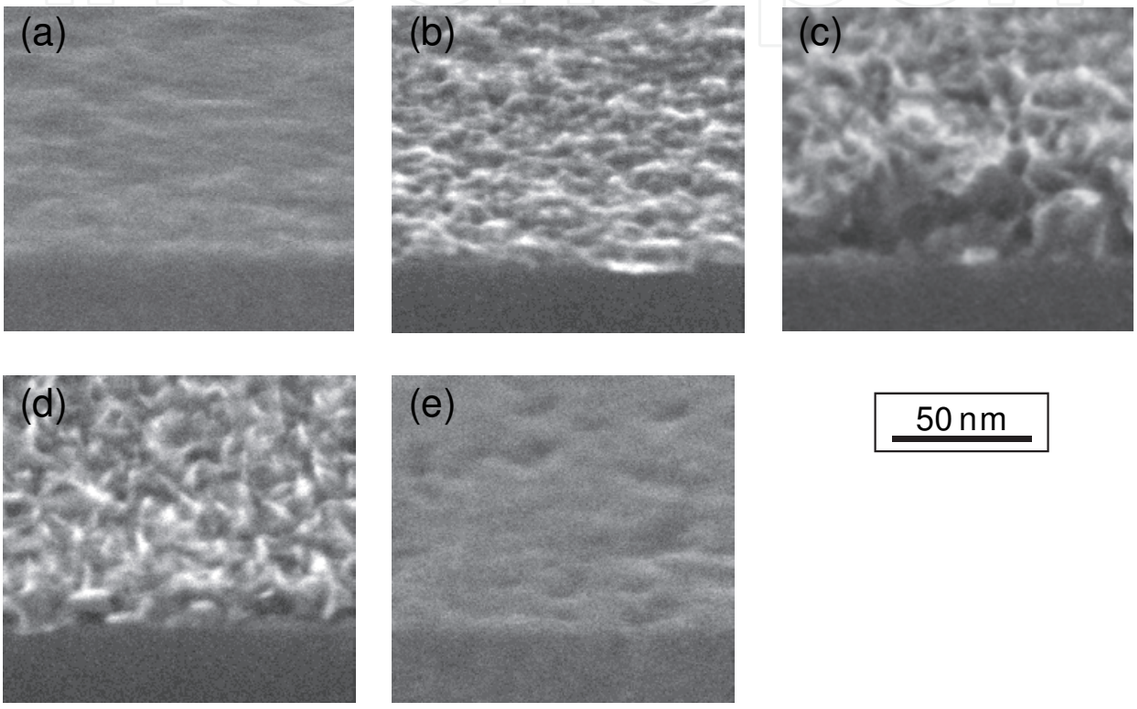


Fig. 6. Tilted-view SEM images of samples synthesized for 35 min at H_2 gas flow rates of (a) 0, (b) 3, (c) 5, (d) 7, and (e) 10 sccm.

Figure 7 shows the variation of CNW height measured from the cross-sectional SEM images as a function of the H_2 gas flow rate. The height of CNWs increased with the H_2 gas flow rate. The highest CNWs (approximately 48 nm) were obtained at a H_2 gas flow rate of 5 sccm. Further increase of the H_2 gas flow rate resulted in a decrease of the CNW height. It should be noted that at H_2 gas flow rates greater than 10 sccm, CNWs were etched, which was confirmed by the following experiment: CNWs were synthesized in advance at a H_2 gas flow rate of 7 sccm (as shown in Figs. 6(d)), and the substrate with CNWs was again introduced into the multi-beam system. H radicals (H_2: 10 sccm or more) and other species (C_2F_6 at 10 sccm, Ar at 5 sccm and accelerated at 200 eV) were irradiated onto the CNW sample. As a result, the height of the CNWs was reduced with increase in the process time. The very thin layer evident in Fig 6(e) was probably deposited when all irradiation was ceased and the conditions of each species would change for just a moment.

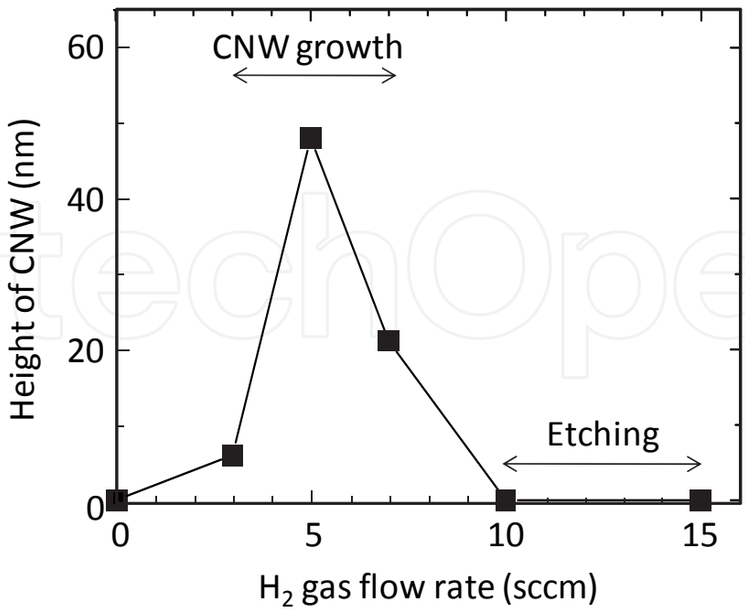


Fig. 7. Height of CNWs as a function of the H_2 gas flow rate.

Vacuum ultraviolet absorption spectroscopy (VUVAS) was applied to measure the absolute density of H radicals during simultaneous irradiation with CF_X radicals, H radicals, and Ar^+ ions.[18-20] The procedure to estimate the H radical density was described in detail in ref. 17-19. Figure 8 shows that the H radical density increased almost linearly with the H_2 gas flow rate, and the highest density of 4.3×10^{11} cm^{-3} was obtained at a H_2 gas flow rate of 7 sccm.

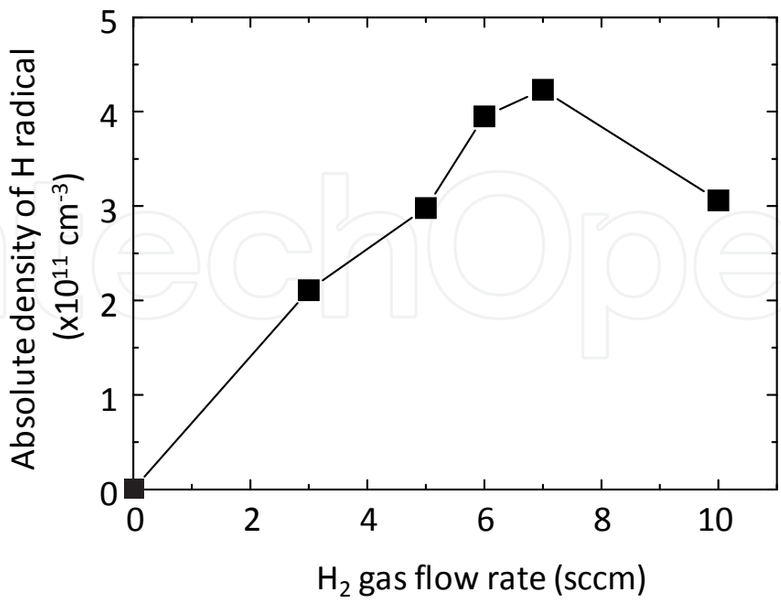


Fig. 8. Absolute density of H radicals as a function of the H_2 gas flow rate measured using VUVAS.

However, the H radical density appeared to decrease with further increase of the H_2 gas flow rate above 7 sccm, which was rather due to the device limitation; it was difficult to efficiently maintain ICP at high flow rates and high pressures. The results shown in Figs. 6–8 suggest that the H radical density has a strong influence on the nucleation and morphology of the resulting CNWs, and there would be an optimum ratio of H radical density to fluorocarbon flux or other species. Moreover, it is noted that CNWs were not formed at a H_2 gas flow rate of 10 sccm, although the H radical density was almost the same as that at 5 sccm. It is presumed that in the case of high flow rate of H_2 gas, the dissociation rate from H_2 molecules to H atoms was low and/or by-products containing H, such as HF and CH_x, were generated. Under such conditions, H_2 molecules would disturb the transport of other important species and chemical reactions. In addition, by-products related to H would influence the amount of CF_x radicals present, which has an important role for CNW growth when using a fluorocarbon/hydrogen system. Therefore, further investigation regarding the role of H_2 molecules is required.

2.3.2 Compositional dependence of CNWs on H radicals

Figure 9 shows atomic composition ratios measured by XPS for CNWs grown at different H_2 flow rates during a simultaneous irradiation process. The composition ratios of F/C and Si/C were estimated from the intensities of the C 1s, F 1s, and Si 2p peaks using ionization cross-section value of each peak. It should be noted that difference in electron inelastic mean free path of each photoelectron and that in surface roughness are not considered at this estimation. Therefore, although absolute values of estimated composition ratios are not precise, qualitative tendencies can be discussed based on them.

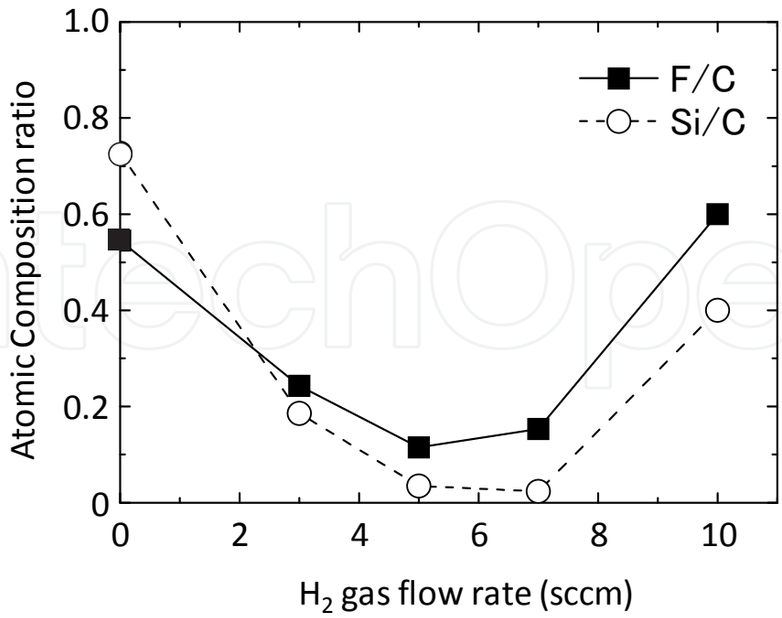


Fig. 9. Atomic composition ratios of CNWs grown at different H_2 flow rates. The flow rates of C_2F_6 and Ar were 10 and 5 sccm, respectively.

At H_2 gas flow rates of 5–7 sccm, where CNWs were definitely formed, a large amount of C was contained mainly in the deposits, while F and Si were rarely detected, which indicates that the Si substrate was fully covered with carbon nanostructures, despite irradiation with fluorocarbon radicals. On the other hand, even when CNWs were not obtained (H_2 gas flow rates of 0 and 10 sccm), F and C were detected, which suggests that a fluorocarbon monolayer is present on the Si substrates. There is also a correlation between the heights of the CNWs shown in Fig.7 and the F contents in the deposits; CNWs with increased height contain lower F content. It is well known that H atoms scavenge F atoms, which results in the formation of by-products such as HF. CNWs were rarely formed at a low H_2 flow rate of 3 sccm or less, because F atoms on the top of the growing CNWs were not sufficiently scavenged. In contrast, CNWs were not formed at a high density of H atoms, because excess H atoms would remove both F and C atoms from the growth surface. Even when CNWs were grown at H_2 gas flow rates of 5–7 sccm, not all F atoms were scavenged, which suggests that other parameters, such as the acceleration voltage, flux of Ar^+ ions, and the surface temperature require optimization.

2.4 Effects of ions on CNW growth

The effects of ions on CNW growth were investigated in a multi-beam CVD system. A first subject is what type of combination of radicals and ions is effective on the initial growth of CNWs. Various combinations of radicals and ions were employed to the first-step at the two-step growth. Secondly, dependence of CNW growth on energy and flux of ions are discussed. Energy and flux of ions during the second step were varied, and changes in surface morphologies of deposits are studied.

2.4.1 Synergetic effects of radicals and ions on CNW growth

The combinations of irradiation species used in the pretreatment step were varied. The pretreatment step consisted of irradiation with Ar^+ ions and/or fluorocarbon radicals and/or H radicals. In all samples, in situ ellipsometry revealed that CNWs were not obtained only by the pretreatment step. The CNW growth process was then carried out for 35 min after pretreatment without exposure to the atmosphere between the pretreatment and CNW growth steps.

Figure 10 shows tilted-view SEM images of the samples after the pretreatment and the CNW growth processes. In Fig. 10, pretreatments were composed of irradiation with (a) energetic Ar^+ ions at 200 eV (Ar^+), (b) CF_3 radicals (CF_3), (c) H radicals (H), (d) $Ar^+ + CF_3$, (e) $Ar^+ + H$, (f) $CF_3 + H$, and (g) $Ar^+ + CF_3 + H$. The conditions for the CNW growth process (second step) were constant for all samples. As shown in Figs. 10(b), (c), and (f), no CNWs were observed, but a thin film was obtained after the CNW growth process with pretreatments consisting of CF_3, H, and $CF_3 + H$. In contrast, CNWs were successfully formed on the Si substrates after CNW growth with pretreatments of Ar^+, $Ar^+ + CF_3$, $Ar^+ + H$, and $Ar^+ + CF_3 + H$, as shown in Figs. 10(a), (d), (e), and (g), respectively. It is noted that CNWs were formed only when irradiation with Ar^+ ions was included in the pretreatment. The CNW heights were different for each sample; however, it is not meaningful to estimate the growth rate, due to the different starting time of CNW growth. In contrast, the morphologies were almost the same when CNWs were obtained, as shown in Figs 10(a), (d), (e), and (g). From SEM observations, it is considered that irradiation with Ar^+ is crucial for subsequent CNW growth; irradiation with Ar^+ is one of the key factors for the formation of Si substrate conditions ideal for CNW growth.

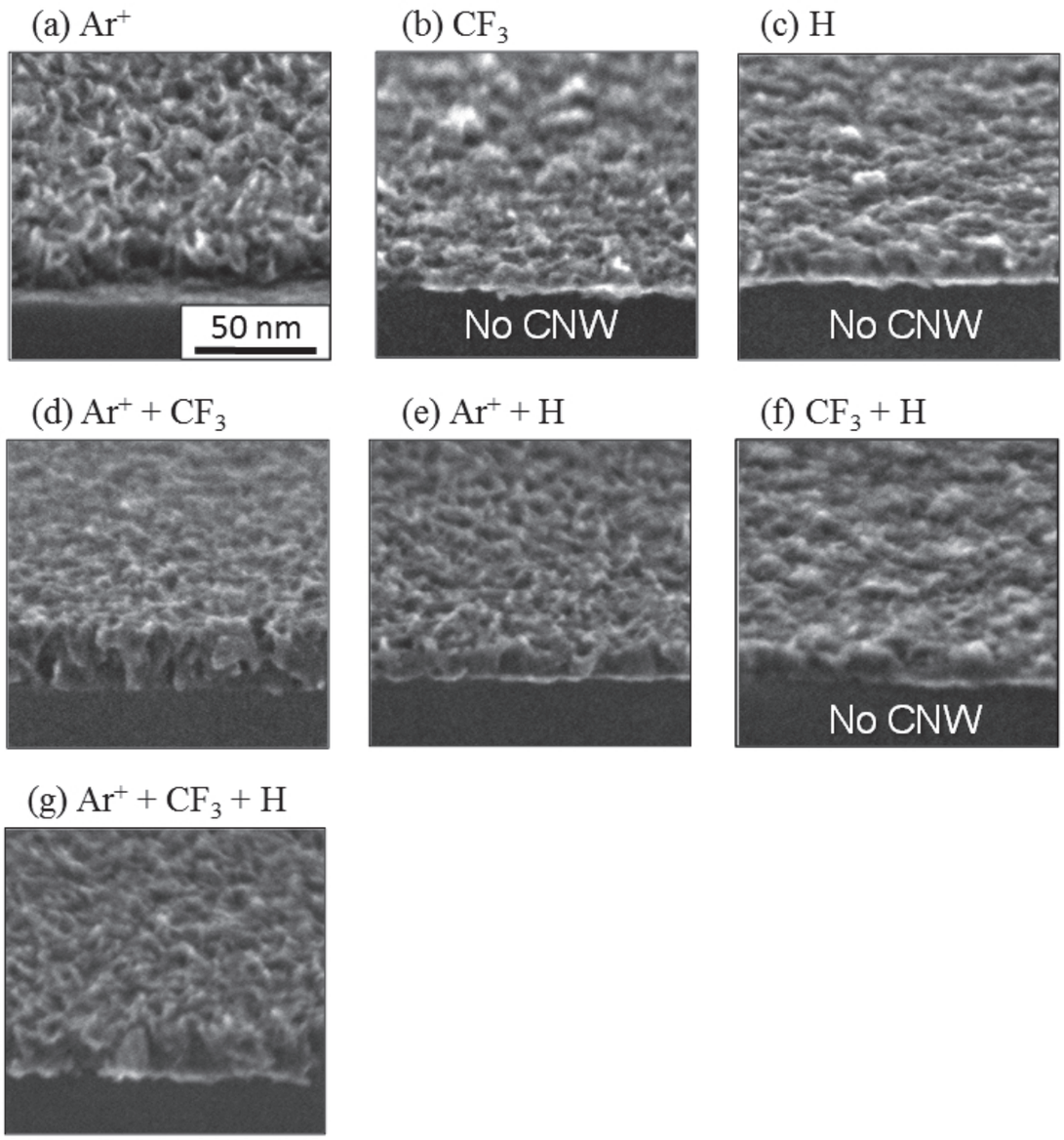


Fig. 10. Tilted-view SEM images of samples after two-step growth on Si substrates. The pretreatment step consisted of irradiation with (a) energetic Ar^+ ions at 200 eV (Ar^+) (b) CF_3 radicals (CF_3), (c) H radicals (H), (d) $Ar^+ + CF_3$, (e) $Ar^+ + H$, (f) $CF_3 + H$, and (g) $Ar^+ + CF_3 + H$. The conditions for the second step (CNW growth) were constant for all samples.

2.4.2 Dependence of CNW growth on energy and flux of ions

Figure 11 shows a chart of Ar^+ ion irradiation and the effect on CNW growth in terms of fluxes ranging from 1.8 to 5.4 μA/cm² and energies ranging from 160 to 250 eV. The variation in morphology is classified in three areas in the chart; CNW formation, continuous film formation, and no deposition, as indicated in Fig. 10 by dark gray, light gray and white backgrounds, respectively. In this figure, heights (h) of grown films are also indicated. At an

Ar^+ ion energy of 200 eV, the heights of grown films increase with increasing the Ar^+ ion flux. This means absorption enhancement of CF_3 radicals by ion irradiation. It is deduced that the ion flux determines the amount of dangling bonds produced on the growth surface. The rate of dangling bond production should be lower than the rate of nucleation site production in order to induce vertical growth of nanographene sheets and result in CNW growth. On the other hand, at an Ar^+ ion flux of 3.8 μA/cm², the heights of grown films decrease with increasing the Ar^+ ion energy. This indicates etching effects of the grown films by the ion irradiation. Therefore, the ion energy is also a critical factor for CNW growth, because its strength determines the production of dangling bonds, nucleation, and etching. Therefore, Ar^+ irradiation conditions with limited fluxes (3.3–3.8 μA/cm²) and energies (200–250 eV) along with CF_3 and H densities in the order of 10^{11} cm^{-3} must be critical factors for CNW growth.

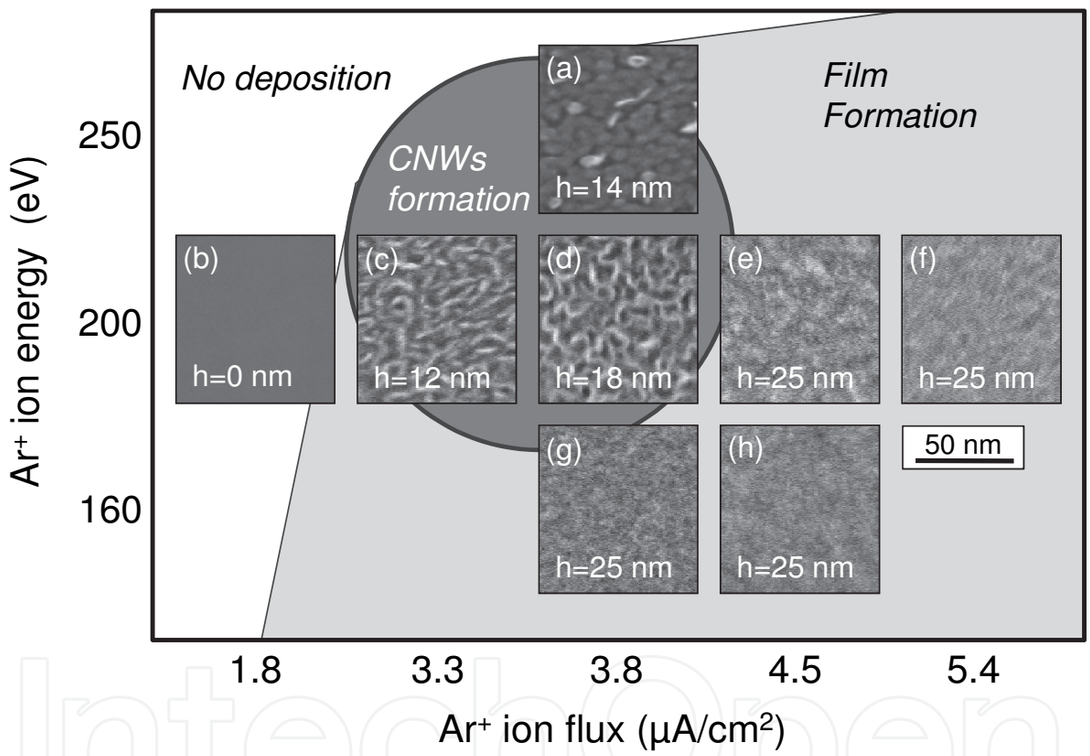


Fig. 11. Chart of Ar^+ ion irradiation for CNW growth for fluxes ranging from 1.8 to 5.4 μA/cm² and ion energies ranging from 160 to 250 eV. The height (h) of each sample is indicated in each SEM image.[13]

The roles of fluorocarbon radicals and hydrogen radicals are discussed. At the top of the growing CNW, the edge would be terminated by CF_3. A H radical migrates to the edge and the terminated F atom at the top is removed by abstraction with a H radical. The HF molecule generated is exhausted to the gas phase. At the same time, dangling bonds are generated on C atoms and CF_3 radicals from the fluorocarbon radical source or migrating on the CNWs are absorbed at the dangling bonds. As a result, a new C-C bond is produced. Repetition of these processes results in CNW growth. It is considered that graphitization would be affected by high energy ion irradiation as well as thermal assist.

In this experiment, the CF_3 density (n_{CF3}) during CNW growth was evaluated to be approximately 4.6–9.2×10^{11} cm^{-3} by QMS. The H radical density (n_H) was evaluated to be approximately 4.0×10^{11} cm^{-3} by VUVAS. These experimental results show n_H/n_{CF3} ranges from 0.4–0.9 when CNWs are grown. Furthermore, three H radicals are needed to abstract all fluorine from a CF_3 molecule. However, since the sticking coefficient of CF_3 radicals to the surface is relatively low, fluorine atoms of absorbed CF_3 radicals would be sufficiently abstracted by H radicals under the present growth conditions with high temperatures.
These fundamental results and discussion are relevant to conventional PECVD methods that employ C_2F_6/H_2 or CH_4/H_2 gases, where mainly CF_x^+ or CH_x^+ ions are irradiated. Details of atomic-level surface reactions at the CNW growth are still under investigation, and further investigations with more accurate experiments are required to solve them. However, it is expected that preferable structures and morphologies of CNWs could be formed through a fundamental understanding of the synergetic effects of the radicals and ions on the chemical reactions at the edges and surfaces of CNWs.

3. Conclusion

Mechanisms of nucleation and vertical growth of nanographenes at the initial growth of CNWs were described in this study. Especially, effects of radicals and ions irradiated to the growth surfaces on the initial growth of CNWs were intensively discussed based on plasma chemistry analyzed by advanced diagnostic techniques.
CNWs were synthesized by irradiation with energetic Ar^+, fluorocarbon and H radicals in a multi-beam CVD system. Fluxes and energies of radicals and ions can be independently controlled. During the initial growth of CNWs, the irradiation conditions required for the nucleation of nanographenes are found to be different from those required for their vertical growth. Ar^+ irradiation is required to form both a-C nanoislands for subsequent nucleation of nanographene on the nanoislands. On Si substrates, SEM observations revealed that irradiation with Ar^+ ions is effective for the initial nucleation process for CNW growth. In addition, irradiation with CF_3 and H radicals is also effective to promote nucleation. From these results, nanoisland formation and CNW growth were successfully distinguished, and the effects of nanoisland formation on nucleation process of nanographene were investigated.
CNWs were successfully synthesized by simultaneous irradiation of CF_X radicals, H radicals, and Ar^+ ions, and it was confirmed that Ar^+ ions were necessary to form CNWs. The growth mechanism and critical factors for CNW growth were quantitatively revealed as follows: low energy Ar^+ cannot induce the nucleation of CNWs, and very high energy Ar^+ enhances the etching of surface carbon atoms. Only under Ar^+ ion irradiation with appropriate energies (200–250 eV) and fluxes (3.3–3.8 μA/cm^2), and with CF_3 and H densities in the order of 10^{11} cm^{-3}, the CNWs are formed. No deposit is found on the substrate without H radical irradiation. With respect to the H_2 gas flow rate, CNWs were grown at 5–7 sccm, where the H radical density was approximately 4.0×10^{11} cm^{-3}. The CF_3 radical density was evaluated by QMS to be approximately 5–9×10^{11} cm^{-3}. XPS results indicated that H radicals also have an important role in the abstraction of F atoms from absorbed CF_3 on CNWs.
These results indicate that a multi-beam CVD system is a powerful tool for fundamental experiments to solve complicated growth mechanisms of carbon nanostructures employing PECVD. Advanced diagnostics of plasma chemistry are also indispensable to make

quantitative discussions about surface reactions during the growth. On the other hand, appropriate plasma conditions necessary for nucleation and vertical growth of nanographenes at the PECVD processes of CNW are determined. It is expected that these results will be very useful for the controlled synthesis of CNWs with preferred morphologies and characteristics.

4. Acknowledgment

This work was partly supported by Ministry of Education, Culture, Sports, Science and Technology, Regional Innovation Cluster Program (Global Type) "Tokai Region Nanotechnology Manufacturing Cluster", Japan.

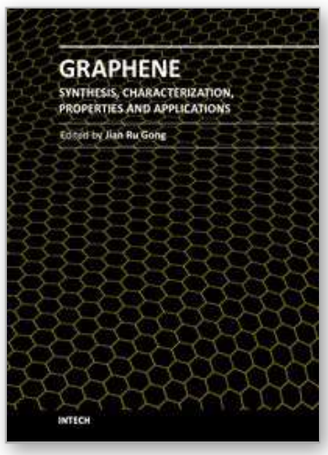
5. References

[1] Iijima, S. (1991). *Nature*, Vol. 354, pp. 56-58.
[2] A. G. Rinzler, J. H. Hafner, P. Nikolaev, L. Lou, S. G. Kim, D. Tomanek, P. Nordlander, D. T. Cobert and R. E. Smalley (1995). *Science*, Vol. 269, pp. 1550-1553.
[3] Seidel, R. V. ; A. P. Graham ; Kretz, J. ; Rajasekharan, B. ; Duesberg, G. S. ; Liebau, M.; Unger, E. ; Kreupl, F. & Hoenlein W. (2005). (2009). *Nano Lett.*, 2005, 5 (1), pp 147–150
[4] Novoselov, K. S.; Geim, A. K.; Morozov, S. V.; Jiang, D.; Zhang, Y.; Dubonos, S. V.; Grigorieva, I. V. & Firsov, A. A. (2004). *Science*, vol. 306, pp. 666-669.
[5] Wu, Y. H. ; Qiao, P. W. ; Chong, T. C. & Shen, Z. X. (2002). *Adv. Mater.,* vol. 14, pp. 64-67.
[6] Hiramatsu, M.; Shiji, K. ; Amano, H. & Hori, M. (2004). *Appl. Phys. Lett.,* vol. 84, pp. 4708-4710.
[7] Takeuchi, W.; Ura, M.; Hiramatsu, M.; Tokuda, Y.; Kano, H. & Hori, M. (2008). *Appl. Phys. Lett.,* vol. 92, pp. 2131031-21310313.
[8] Wang, J. J.; Zhu, M. Y.; Outlaw, R. A.; Zhao, X.; Manos, D. M.; Holloway, B. C. & Mammana, V. P. (2004). *Appl. Phys. Lett.,* vol. 85, pp. 1265-1267.
[9] Sato, G.; Morio, T.; Kato, T. & Hatakeyama, R. (2006). *Jpn. J. Appl. Phys.*, vol. 45, pp. 5210-5212.
[10] Chuanga, A. T. H.; Boskovicb, B. O. & Robertson, J. (2006). *Diamond Relat. Mater.*, vol. 15, pp. 1103-1106.
[11] Kobayashi, K.; Tanimura, M.; Nakai, H.; Yoshimura, A.; Yoshimura, H.; Kojima, K. & Tachibana, M. (2007). *J. Appl. Phys.,* vol. 101, pp. 094306-1-094306-4.
[12] Yoshimura, H.; Yamada, S.; Yoshimura, A.; Hirosawa, I.; Kojimaa, K. & Tachibana, M. (2009). *Chem. Phys. Lett.*, vol. 482, pp. 125-128.
[13] Kondo, S.; Kawai, S.; Hori, M.; Yamakawa, K.; Den, S.; Kano, H. & Hiramatsu, M. (2009). *J. Appl. Phys.,* vol. 106, pp. 094302-1-094302-6.
[14] Kondo, S.; Kondo, H.; Hiramatsu, M.; Sekine, M. & Hori, M. (2010). *Appl. Phys. Expr.*, vol. 3, pp. 045102-1-045102-3
[15] Sugai, H. & Toyota, H. (1992). *J. Vac. Sci. Technol. A*, vol. 10, pp. 1193-1200.
[16] Hikosaka, Y., Nakamura, M. & Sugai, H. (1994). *Jpn. J. Appl. Phys.*, vol. 33, pp. 2157-2163.
[17] Hori, M. & Goto, T. (2002). *Appl. Surf. Sci.*, vol. 192, pp. 135-160.
[18] Takashima, S.; Arai, S.; Hori, M.; Goto, T.; Kono, A.; Ito, M. & Yoneda, K. (2001). *J.Vac.Sci.Technol.*, vol.A19, pp.599-602.

[19] Flaherty, D. W.; Kasper, M. A.; Baio, J. E.; Graves, D. B.; Winters, H. F.; Winstead, C. & McKoy, V. (2006). J. Phys. D: vol. 39, pp.4393-4399.
[20] Takeuchi, W.; Sasaki, H.; Kato, S.; Takashima, S.; Hiramatsu, M. & Hori, M. (2009). *J. Appl. Phys.*, vol. 105, pp. 113305 -1- 113305 -6.

IntechOpen

IntechOpen



Graphene - Synthesis, Characterization, Properties and Applications

Edited by Prof. Jian Gong

ISBN 978-953-307-292-0
Hard cover, 184 pages
Publisher InTech
Published online 15, September, 2011
Published in print edition September, 2011

The discovery of graphene has led to a deluge of international research interest, and this new material in the field of materials science and condensed-matter physics has revealed a cornucopia of new physics and potential applications. This collection gives a roughly review on the recent progress on the synthesis, characterization, properties and applications of graphene, providing useful information for researchers interested in this area.

How to reference

In order to correctly reference this scholarly work, feel free to copy and paste the following:

Hiroki Kondo, Masaru Hori and Mineo Hiramatsu (2011). Nucleation and Vertical Growth of Nano-Graphene Sheets, Graphene - Synthesis, Characterization, Properties and Applications, Prof. Jian Gong (Ed.), ISBN: 978-953-307-292-0, InTech, Available from: http://www.intechopen.com/books/graphene-synthesis-characterization-properties-and-applications/nucleation-and-vertical-growth-of-nano-graphene-sheets

INTECH
open science | open minds

InTech Europe
University Campus STeP Ri
Slavka Krautzeka 83/A
51000 Rijeka, Croatia
Phone: +385 (51) 770 447
Fax: +385 (51) 686 166
www.intechopen.com

InTech China
Unit 405, Office Block, Hotel Equatorial Shanghai
No.65, Yan An Road (West), Shanghai, 200040, China
中国上海市延安西路65号上海国际贵都大饭店办公楼405单元
Phone: +86-21-62489820
Fax: +86-21-62489821

© 2011 The Author(s). Licensee IntechOpen. This chapter is distributed under the terms of the Creative Commons Attribution-NonCommercial-ShareAlike-3.0 License, which permits use, distribution and reproduction for non-commercial purposes, provided the original is properly cited and derivative works building on this content are distributed under the same license.

IntechOpen

IntechOpen